Journal of Physics: Conference Series

PAPER • OPEN ACCESS

Multi-physics model development and application to real-case alkaline electrolyzer

To cite this article: M Dreoni *et al* 2023 *J. Phys.: Conf. Ser.* **2648** 012060

View the article online for updates and enhancements.

You may also like

- Parametric Modelling and Optimization of Alkaline Electrolyzer for the Production of Green Hydrogen
S Niroula, C Chaudhary, A Subedi et al.
- A Multi-Physics Model of Low-Voltage Dual-Electrolyte Water Electrolyzers
Joy Marie Mora, Rinlee Butch Cervera, Joey Duran Ocon et al.
- Deactivation Mechanisms of Atmospheric Plasma Spraying Raney Nickel Electrodes
Daniel Chade, Leonard Berlouis, David Infield et al.

This content was downloaded from IP address 150.217.19.161 on 15/03/2024 at 16:56

Multi-physics model development and application to real-case alkaline electrolyzer

M Dreoni [a], F Balduzzi [a], F M Ferro [b], G Fagioli [b], K Panichi [b], G Ferrara [a] and A Bianchini [a]

[a] Department of Industrial Engineering, Università degli Studi di Firenze, Via di Santa Marta 3, 50139, Firenze, Italy.

[b] McPhy Energy Italia, Via Ayrton Senna 22, 56028, San Miniato, PI, Italy.

Corresponding author: francesco.balduzzi@unifi.it

Abstract. The realization of mathematical, multi-physics models for alkaline electrolyzers is crucial for advancing this technology. Lumped parameter models offer shorter simulation times, compared with other approaches, and practical industrial applications. If electrochemical models provide the polarization curve, the hydrogen production rate, and the device efficiency, thermal models solve the equations involving the electrolyte temperature. With a coupled approach, the two models can be linked together by considering the device voltage as temperature dependent. Despite the relevance of such models, few instances of their direct application on existing electrolyzers can be found in the literature, and combined electrochemical-thermal simulations are rare.
This study presents a multi-physics model applied on an alkaline electrolyzer and validated against measurements acquired on a dedicated experimental test bench.
The physics-based model accurately predicts the polarization curve, exhibiting a high precision match with experimental data. Additionally, it identifies material or geometrical imperfections in the electrolyzer, allowing for optimization in the design phase. The thermal model successfully converges to the desired electrolyte temperature of 72 °C under stationary conditions. Additional transient simulations demonstrate an average deviation of only 0.25% compared to the measured temperature trend. Finally, a sensitivity analysis explores the coupling of the electrolyzer with a wind turbine under different wind conditions.
The study showcases the effectiveness of the coupled electrochemical-thermal model in predicting electrolyzer performance, with a direct application to a wind turbine power output.

Keywords: Electrolyzers, Multi-physics model, Green Hydrogen, Alkaline

1. Introduction and scope of the study

Hydrogen production via electrolysis is one of the possible solutions to the problem of electricity storage linked to the increasing use of renewable sources. In fact, hydrogen can be used as energy carrier and it is well suited to be transported to the utilization point. It is also used in various industrial sectors, such as chemical plants, refineries and steel industries. Due to its utilization in different sectors, the consumption of hydrogen is substantial and is expected to increase in the coming years, necessitating large-scale production. In 2021, the demand for hydrogen reached 94 million tons (Mt), resulting in associated emissions of over 900 Mt CO_2 [1]. This accounts for approximately 2% of global CO_2


Content from this work may be used under the terms of the Creative Commons Attribution 3.0 licence. Any further distribution of this work must maintain attribution to the author(s) and the title of the work, journal citation and DOI.
Published under licence by IOP Publishing Ltd

emissions [2]. The significant carbon footprint is primarily attributed to hydrogen production through steam reforming, whereas water electrolysis contributes only 4% to the overall production [3].

Industrially speaking, the mature technology to produce hydrogen through electrolysis are alkaline electrolyzers. In fact, the working conditions at low temperatures, 70÷90 °C, and the use of electrolytic solutions of KOH and NaOH allow to employ inexpensive materials within the devices.

One of the necessary phases for the advancement of this technology is the development of reliable and physics-based mathematical models for electrolyzer simulation. In fact, lumped parameter models enable the simulation of a device through simplified resolution of the underlying physical equations governing the technology. Using this approach, the design phase can speed up, since there is no need for physical experimentation. Furthermore, modeling plays a crucial role in addressing the dynamic challenges of connecting intermittent electrical sources to electrolyzers, as in renewable hydrogen energy systems (RHES). It helps understanding the phenomena involved and enables control analysis, proper sizing of components, energy management and the overall optimization of the process.

The scope of this paper is to present the application of a coupled electrochemical-thermodynamic model on an alkaline electrolyzer produced by McPhy company. The model was implemented using Matlab® environment and validated against measurements acquired on a dedicated experimental test bench. The authors first conducted a literature review of the current electrolysis modeling state-of-the-art, identifying recent works of different complexity.

The paper is divided into four main sections. Chapter 2 presents the electrolysis models employed, from the electrochemical and thermal points of view, after a brief overview on the state-of-the-art from the literature. Chapter 3 illustrates the electrolyzer employed as case study and, finally, the Chapter 4 and Chapter 5 are dedicated to showing the models setup, results and conclusions.

2. Electrolysis model

Lumped parameter models have become increasingly popular in all engineering fields with the advantages over costly experiments, such as time reduction, more efficient equipment design and optimization of operating conditions. For this reason, this modeling approach is spreading in industries and research. In particular, for electrolyzers, the first models were developed starting from the end of 20th century although alkaline electrolyzers had already been industrialized for several years.

The following paragraph is a brief overview of the models found in the literature.

2.1. Literature review of modeling approaches

Electrochemical models of electrolyzers provide three main outputs:

1. Polarization curve.
2. Amount of hydrogen produced.
3. Device efficiency.

There are various approaches to modeling with the most direct one being a linear model. The model employed by Gutiérrez-Martín et al. describes the cell potential as a linear function of the current [4], while a model with dependence on temperature and pressure was used by Ursúa and Sanchis [5] and Sarrias-Mena et al. [6]. The last authors investigated four different options of electrical models for an efficient characterization of RHES.

Models involving a larger number of physical effects are the empirical ones, such as the one employed by Tijani et al. [7] or by Vanhanen et al. [8] who employed semi-empirical coefficients by fitting current-voltage curves, obtained experimentally. In this context, a trade-off between simple and complex modeling was used in the much-cited paper by Ulleberg et al. [9]. The main drawback of empirical models depends on the fact that they are case-dependent with need for calibration of constants.

Linear and empirical models often rely only on temperature as operating parameter, without being comprehensive. Consequently, the impact of other variables, e.g. pressure, concentrations and bubbling rate, on electrolyte and electrodes is neglected. In this context, more complex, physics-based models

were developed, such as the one used by Zeng et al. [10], with an insight on kinetics, Henao et al. [11] and Hammoudi et al. [12].

Together with the electrochemical model, a thermal characterization of the system was employed by Ulleberg et al. [9], Hammoudi et al. [12] and Deshmukh et al. [13]. Principles of accumulation, exchange and generation of heat aim to provide the evolution of the electrolyte temperature as a function of the current supplied to the system.

For a more comprehensive study on the main models employed for low temperature electrolyzers, it is suggested by the authors to have a look at the work by Olivier et al. [14].

2.2. Physics-based model

The focus of this study was the development of a physics-based model, including thermodynamic and two-phase effects and coupled to a thermal model. Inspiration was taken from the paper by Hammoudi et al. [12], aiming to achieve a better estimation of power consumption and amount of hydrogen production, based on the physical state of the electrolyzer. Also, it is able to improve the electrolyzer management, by enabling better control and monitoring of the system. Finally, it is a useful approach when electrolysis is powered by intermittent sources of energy, as wind or solar energy.

2.2.1 Polarization curve and thermodynamic approach

The polarization curve is the characteristic graph of the electrolyzer, showing the variation of its cell potential in relation to current density. The basic equation of electrolysis to express the cell potential is:

$$U = U_{rev} + U_{act} + U_{conc} + U_{ohm}\,, \tag{1}$$

where U_{rev} is the reversible potential of the cell, U_{act} is the activation overpotential, U_{conc} is the concentration overpotential and U_{ohm} is the ohmic component, related to the electrical resistances. Each polarization represents a source of loss in efficiency. In Figure 1 the contribution of the overpotentials to the curve is highlighted (source Amores et al. [15]).

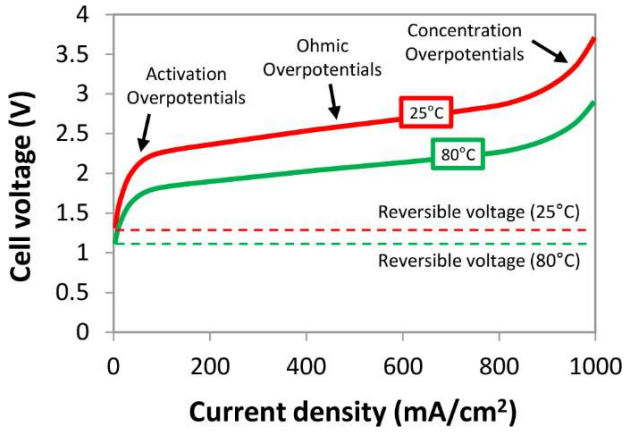

Figure 1. Example of polarization curves at different temperatures [15].

The impact of concentration overpotential becomes significant at higher current densities compared to those in the case study, making it negligible for the current analysis. From a commercial standpoint, it might be worthwhile to consider operating at current densities beyond the usual values. In such a scenario, incorporating U_{conc} into the model would be necessary. A possible definition of U_{conc} can be found in [16]:

$$U_{conc} = \frac{RT}{nF} ln\left(1 - \frac{i}{i_1}\right), \tag{2}$$

where R is the gas constant, T is the temperature, n is the number of electrons involved, F is Faraday's constant, i is the current density and i_1 is the maximum rate of current density.

U_{rev} was obtained through Nernst equation, as in [17], with a thermodynamic approach including thermal and barometric effects:

$$U_{rev} = U^0{}_{rev} + \frac{RT}{nF} ln\left((p - p_w)^{1.5} \frac{p_{w^*}}{p_w}\right), \tag{3}$$

where $U^0{}_{rev}$ is the reversible potential in standard conditions, whereas p, p_w, p_{w^*} are respectively the partial pressures of the gas, of water vapor and of water vapor at standard temperature. The last two properties were obtained from Le Roy [17]:

$$p_w = T^{-3.498}\, exp\left(37.93 - \frac{6426.32}{T}\right) exp\left(0.016214 - 0.13802m + 0.19330\sqrt{m}\right), \tag{4}$$

$$p_{w^*} = T^{-3.4159} ex\, p\left(37.43 - \frac{6275.7}{T}\right), \tag{5}$$

where m represents the electrolyte molarity.

For the activation overpotential of anode and cathode $U_{act_{a/c}}$, Tafel equation was employed [12]:

$$U_{ac\ a/c} = 2.3026 \frac{RT}{nF\alpha_{a/c}} ln\left(\frac{i}{i_{0\,a/c}}\right), \tag{6}$$

where $i_{0\,a/c}$ are the exchange current densities for anode and cathode and $\alpha_{a/c}$ are anode and cathode transfer-charge coefficients, defined with the Nickel electrode correlation [12]:

$$\alpha_a = 0.0675 + 0.000095T, \tag{7}$$

$$\alpha_c = 0.1175 + 0.000095T. \tag{8}$$

Regarding the ohmic component, U_{ohm}, Ohm's law was applied to account for the resistances of anode, R_a, cathode, R_c, electrolyte and membrane, $R_{membrane}$. In this case, having a zero-gap electrolyzer, the contribute of the electrolyte could be neglected, leading to the following equation:

$$U_{ohm} = (R_a + R_c + R_{membrane})\, i. \tag{9}$$

Ohm's second law was used for anode and cathode contributions, whereas the membrane resistivity was provided by the supplier. The formulation of a T-dependent membrane resistance, from Henao et al. [11], was also taken into consideration for a sensitivity analysis on the model:

$$R_{membrane} = (0.06 + 80 \exp(T/50))/(10{,}000\, A), \tag{10}$$

where A is the membrane surface in cm² and T is the electrolyte temperature, in °C.

2.2.2 Two-phase effects

The model also considers two-phase effects. In particular, the bubble generation at cathode and anode affects the current density and the overall potential, through bubble coverage of the effective electrode surface. To account for this effect, a variable θ linked to area reduction was defined as follows [18]:

$$\theta = \left(\frac{\mathrm{i}}{i_{\mathrm{lim}}}\right)^{0.3}, \tag{11}$$

where i_{lim} is a maximum current density, imposed conventionally as 300,000 A/m².

2.2.3 Device efficiency

Finally, the device efficiency η was defined. The efficiency of an alkaline electrolyzer can be described in terms of its electrical efficiency and its overall efficiency. The first one is the ratio of the electrical energy used for the electrolysis process to the lower heating value (LHV) of the hydrogen gas produced. The second one includes all energy losses associated with the electrolysis process, including heat losses and other auxiliary energy requirements. Overall efficiency can be lower than electrical efficiency and is affected by various factors such as operating temperature, pressure, current density, and the purity of the input water.

In the present study a Faradic efficiency was however taken into account, as follows [12]:

$$\eta = \frac{U_{rev}}{U}. \tag{12}$$

Faradaic efficiency is a critical performance metric used to evaluate the effectiveness of an electrolyzer in terms of converting electrical energy into the desired chemical reaction.

2.3. Thermal model

The thermal aspect is another crucial factor in simulating an electrolyzer. Electrochemical and thermal models are intricately connected, as the cell voltage impacts the electrolyte temperature, which in turn influences the electrical parameters. Monitoring the electrolyte temperature allows for proper sizing of the cooling system and it is fundamental in partial, discontinuous operation (as in case of coupling with renewable sources) or during start-up. Also, the thermodynamic aspect must be monitored for mechanical needs. In fact, it is desirable that the electrolyte temperature is as high as possible to improve the electrolyzer performance, but within the material limits.

In the present study, the approach outlined in [12] was followed and the equation below was considered to obtain the electrolyte temperature:

$$C\frac{dT}{dt} = Q_{gen} + Q_{exch} + Q_{loss} + Q_{cooling}\,, \tag{13}$$

where C represents the thermal capacity, T the electrolyte temperature, Q_{ge} the heat generated due to chemical reactions, Q_{exch} the heat exchanged through mass transfers, Q_{loss} the heat dissipated through convection and conduction and $Q_{cooling}$ the thermal energy removed by the cooling system. Q_{gen} depends on the thermoneutral potential U_{th} and it is calculated with the following equation:

$$Q_{gen} = N_C(U - U_{th})\,I, \tag{14}$$

where N_C is the number of cells in series per stack and U is the electrolyzer cell voltage.

Q_{exch} and Q_{loss} can be defined as follows:

$$Q_{exch} = \sum_{i=1}^{N} \dot{m}_{\mathrm{i}} c_{p_{\mathrm{i}}} \Delta T\,, \tag{15}$$

$$Q_{loss} = (T - T_{amb})/R_{th}\,, \tag{16}$$

where $\dot{m}_{\mathrm{i}}$ is the mass-flow of the i-th mass flux, $c_{p_{\mathrm{i}}}$ is the i-th specific heat, ΔT the difference of temperature due to the heat exchange, T_{amb} is the external temperature and R_{th} is the total thermal resistance, composed of conductive and convective resistances, expressed as:

$$R_{th} = \ln\left(\frac{r_{ext}}{r_{int}}\right) / \,(2\,\pi\,L\,\lambda) + 1/(hA_{ext})\,, \tag{17}$$

being λ and h the conduction and convection coefficients.

Finally, $Q_{cooling}$ can be modeled through heat exchangers equation:

$$Q_{cooling} = U_{th}\, A\, \Delta T_{ml}\,, \tag{18}$$

where U_{th} is the global heat exchange coefficient, A the heat surface and ΔT_{ml} the logarithmic mean temperature difference, defined as follows:

$$\Delta T_{ml} = \frac{\Delta T_{in} - \Delta T_{out}}{\ln(\Delta T_{in}/\Delta T_{out})}, \tag{19}$$

where the subscripts "in" and "out" represent the inlet and outlet sections of the flows. The product $U_{th}A$ is generally known, dependent on the geometry and materials of the heat exchanger, and can be easily found on the heat exchanger catalogue.

The whole electrolyzer plant was simplified to three main components: the stack, i.e. the core of the system where electrolysis takes place, and two separators where the produced gases leave the system and the electrolyte is refrigerated to enter the stack at the correct temperature, i.e. 60 °C, below which the cooling system does not activate. The temperature inside the stack is kept around 70÷80 °C, thanks to the supplied electrolyte flow. Figure 2 shows the functional diagram of the stack-separators system, where the main flows are indicated, as well as the control volumes for the components analyzed: green-squared volumes for the separators and red ones for the stack.

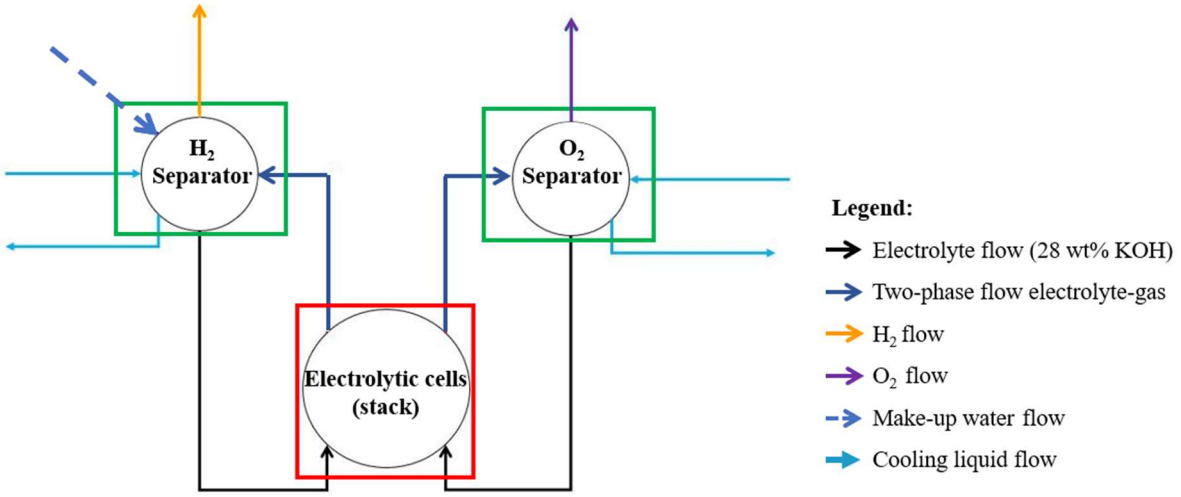

Figure 2. Functional diagram of stack and separators system.

As a first step, the stack was individually modeled. Since only the separators are refrigerated, it was necessary to adapt the model described in the previous paragraph by modifying the differential equation (13) to the simplified equation:

$$C_{stack}\frac{dT_{stack}}{dt} = Q_{gen_{stack}} - Q_{exch_{stack}} - Q_{loss_{stack}}. \tag{20}$$

The heat capacity of the stack, C_{stack}, was calculated considering the nominal capacity of the stack and the flow rates of H_2 and O_2 were determined using Faraday's equation. Regarding the heat dissipated by the stack to the environment, it was found according to conduction and convection laws, by using the geometrical and material-related data available.

The simulation of the two separators is the same, except for the make-up water flow rate, which is only introduced in H_2 separator to compensate the water lost through chemical reaction.

Once more, it was necessary to modify equation (13) to adapt it to the specific case. In fact, the contribution of the heat generated by the chemical reaction of electrolysis can be omitted, while it is necessary to consider the heat removed by the cooling system:

$$C_{sep}\frac{dT_{sep}}{dt} = Q_{exch_{sep}} - Q_{loss_{sep}} - Q_{cooling_{sep}}. \quad (21)$$

The flow of electrolyte from the stack has a higher temperature than the flow exiting the separator. Equation (15) was then modified as follows:

$$Q_{exch_{sep}} = \dot{m}_{ele_{ric}} C_{p_{ele_{ric}}} \Delta T_{ele_{ric}} + \dot{m}_{H_2} C_{p_{H_2}} \Delta T_{H_2} + \dot{m}_{H_2O} C_{p_{H_2O}} \Delta T_{H_2O}\ , \quad (22)$$

being the last term only employed for H_2 separator, where the make-up water is introduced. A maximum value for the electrolyte flow rate was defined while the minimum recirculation flow rate was set to 30% of the total flow rate, according to the installed pump.

3. Case study

The model described in the previous chapter was applied to a small-size, zero-gap, alkaline electrolyzer produced by McPhy, namely the "McLyzer 20-30®". For this device, the electrolyte is an aqueous solution of potassium hydroxide 28 wt% KOH, whereas the electrodes are in nickel. Table 1 describes the main characteristics of the electrolyzer:

Table 1. Electrolyzer characteristics.

Cells number	65
Pressure	1÷30 bar
Power	100 kW
Hydrogen production (nominal flow rate)	20 Nm^3/h
Design Temperature	80 °C
Membrane resistivity	0.10 $\Omega \cdot cm^2$
Nickel conductivity	1.4 x10^7 S/m

As already said, material compatibility is a reason why the electrolyte temperature must be carefully monitored. The acceptable temperature range for the case study is between 70 and 80 °C, due to the electrolyte conductivity that reaches its maximum around these values. However, the real temperature limit is given by the membrane, which maintains its electrolyte permeability characteristics only for temperatures below 80÷100 °C.

The electrolyzer underwent two distinct experimental campaigns to calibrate and verify the accuracy of the model. The first campaign focused on validating the I -V curve of the electrochemical model. In the second campaign, the reliability of the thermal model was evaluated using a transient approach. This involved varying the current over time at the test bench, using the values outlined in Table 2 below.

Table 2. Current supplied to the device vs time

Time [min]	Current [A]
0÷20	0 A
20÷30	425 A
30÷40	605 A

Additional sensitivity analyses were performed on the model to experience the validity of the physics-based model, whose strength is the independence from real-case electrolyzers. To examine the electrochemical aspects, variations were made to the membrane resistance to observe the corresponding output in terms of polarization curve. For what concerns the thermal model, a case of variable current with time was simulated, namely the power output data derived from a wind turbine.

4. Results

4.1. Physics-based electrochemical model results

Using the electrochemical model described in Chapter 2, the polarization curve was obtained, which outputs the voltage values given the input current to the system. Due to confidentiality reasons, the potential values on the y-axis will not be shown. The graph obtained was then compared to the experimental data, as shown below. It was immediately evident how the curve obtained from the model had a different trend from that of the data (Figure 3a). In particular, the discrepancy is evident in the zone with higher current values (error of about 10%).

To identify potential inaccuracies within the model, a detailed examination was conducted on the individual components contributing to the overall voltage of the curve. Specifically, the activation and ohmic overpotentials were analyzed. The activation overpotential demonstrates a logarithmic trend and tends to stabilize for higher current densities. On the other hand, the ohmic component is directly proportional to the supplied current and includes the combined resistances of the electrodes and membrane. The material of the membrane was identified as the critical element through a dedicated test bench and assessed as a source of greater overvoltage, due to premature deterioration. Consequently, the resistance of the membrane was increased based on experimental considerations, obtaining the following result (Figure 3b).

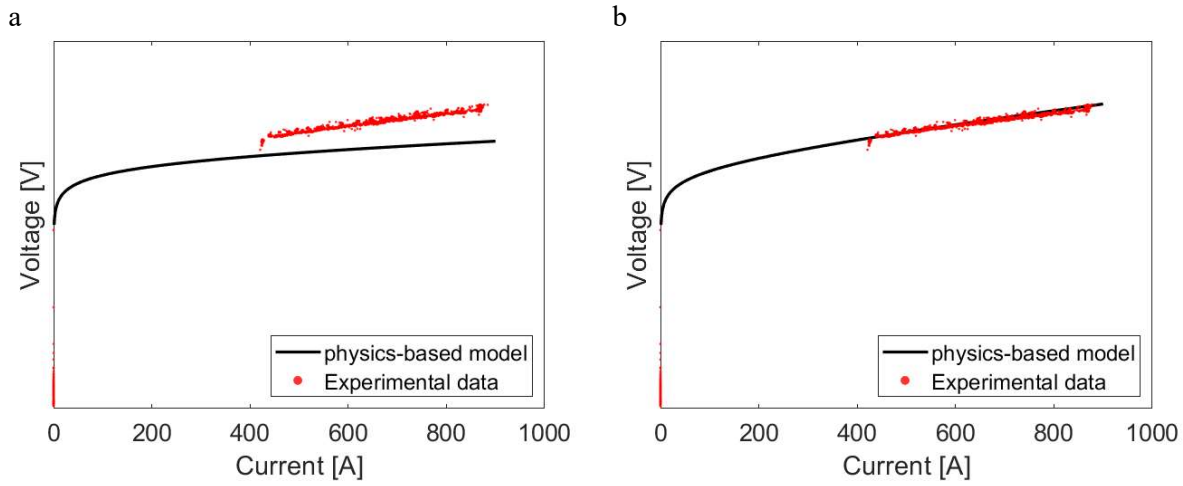

Figure 3. Polarization curve: comparison between measurements and numerical model. (a) Model with original value of membrane resistance. (b) Model with modified value of membrane resistance.

The results obtained, as highlighted by the graphs, demonstrate an excellent resolution for the model (R^2 about 0.9).

4.2. Sensitivity analysis on the membrane resistivity

Having assessed the reliability of the electrochemical model, a sensitivity analysis was conducted, by analyzing the impact of the membrane resistivity as a key parameter. Thanks to the physics-based modeling, materials and geometry can be changed to evaluate how the overall simulation performs, without the need for a real-case device to be tested.

The resistivity value was changed from a low one (r=0.1 $\Omega \cdot cm^2$), typical of a membrane in good state, to a higher one (r=0.8 $\Omega \cdot cm^2$), representative of a degraded membrane. The formulation of Henao (equation 10) was also considered for the sensitivity analysis. The results are shown in the graph below.

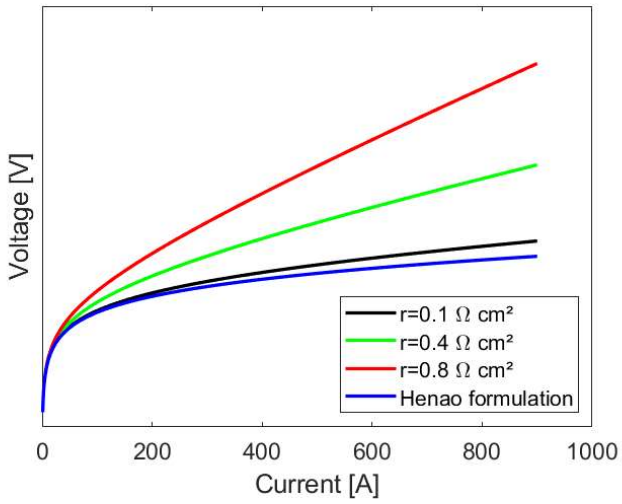

Figure 4. Membrane resistivity analysis: impact on the I -V curve.

The impact of the diaphragm resistivity is clear and must be carefully selected. Henao formulation, depending on the electrolyte temperature, was here used based on a constant temperature of 80 °C. It appeared to be, anyway, too optimistic, with a resistivity even lower than 0.1 $\Omega \cdot cm^2$.

4.3. Thermodynamic model setup and results

The thermodynamic model described in Chapter 2 was applied to the system including the electrolyzer and the separators of hydrogen and oxygen. Having defined the model of the stack from a geometrical point of view, operational inputs were given, as initial conditions. External temperature was set to 25 °C, electrolyte inlet temperature to 60 °C and initial stack temperature to 60 °C.

First of all, a result of the temperature trend for the individual modeling of the stack was obtained. The value of temperature, as function of time, is displayed in the graph below (Figure 5a). When reaching steady-state conditions, the model returns an electrolyte temperature of around 72 °C, which corresponds to the operating data of the tested device when the nominal input current is applied.

Once the separators and the stack were modeled, it was possible to connect them to simulate the whole system from a thermal point of view. The model was validated by taking into account intermittent operating data according to the test reported in Table 2. In the initial state of the time-dependent test the electrolyzer was operating at design conditions. At t = 0 s the power was switched off for 20 min, and then the input current was progressively increased in two steps. The result related to the electrolyte temperature trend is displayed in the graph below (Figure 5b), where it is compared to the analogous experimental measurements.

The average deviation between the two data sets is about 0.25%, suggesting that the model accurately simulates the behavior of the device also during transient operation.

4.4. Thermal response and hydrogen production with intermittent source of renewable power

The thermal model was applied to available data sets coming from a wind turbine with nominal power comparable to the one of the electrolyzer (160 kW), thus suitable for a coupling of the two energy systems. Two different days of wind energy production were evaluated: a windy day, characterized by a large amount of power available, and an average, less windy, day, with medium production. A minimum power cut-off was imposed: the electrolyzer was switched off in all cases corresponding to an input power of less than 20% of the nominal power. And, on the other hand, the maximum peaks were managed so that the power supplied to the electrolyzer could not exceed the nominal one.

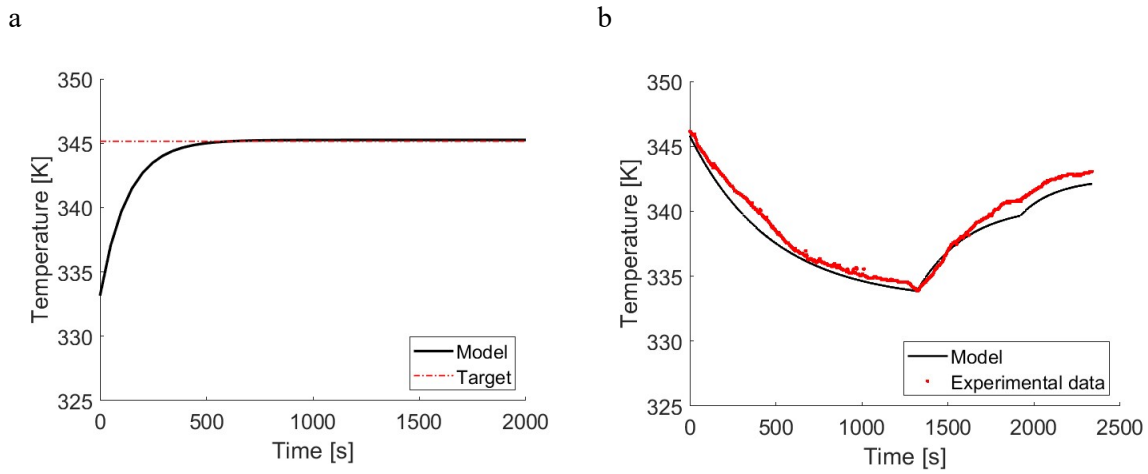

Figure 5. (a) Simulation of the steady-state operation of the stack. (b) Electrolyte transient temperature: comparison between the collected data and the system thermal modeling

The designed Matlab® code requires a first initialization with a linear approximation of the polarization curve, to have initial values of current and voltage starting from the values of the wind power provided. A first guess of the stack temperature is then obtained and employed for the physical model involving electrochemistry. Using the overpotential equations it is then possible to obtain a more precise value of voltage and current that can be used to re-initialize the calculus, iteratively. The electrolyte temperature trend for the two cases is reported in the graphs below, together with the actual instantaneous power generated by the wind turbine.

The temperature effectively follows the peaks of power, with a slight delay and damping, with respect to the sharp variation of current, due to the thermal inertia of the system. This result confirms the good behavior of the model although having a constant electrolyte temperature inside the stack would be more suitable in terms of efficiency. To ensure a stable temperature at the design value, attention must be given to optimizing the turbine-electrolyzer coupling, and the sizing of separators will also have a significant impact as they act as thermal buffers.

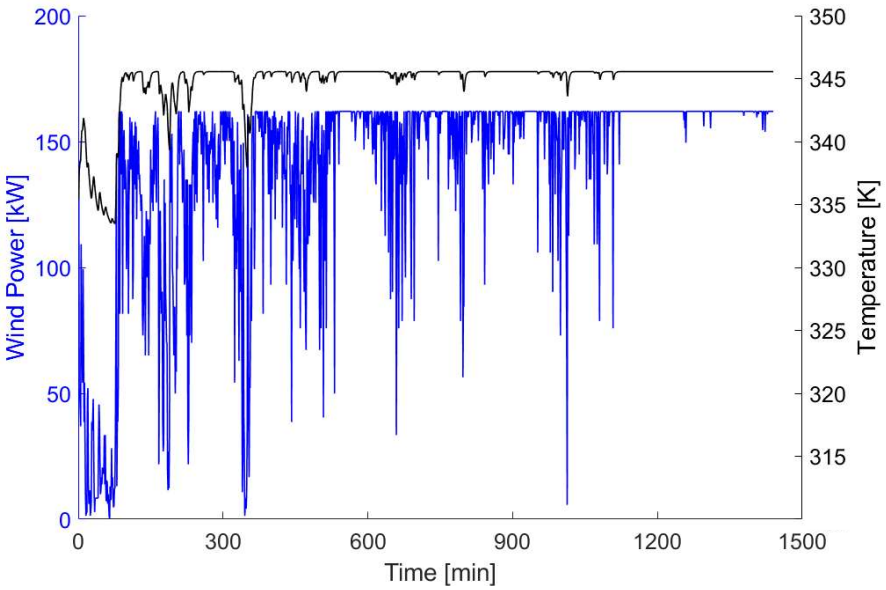

Figure 6. Power from a wind turbine and respective temperature trend during a windy day.

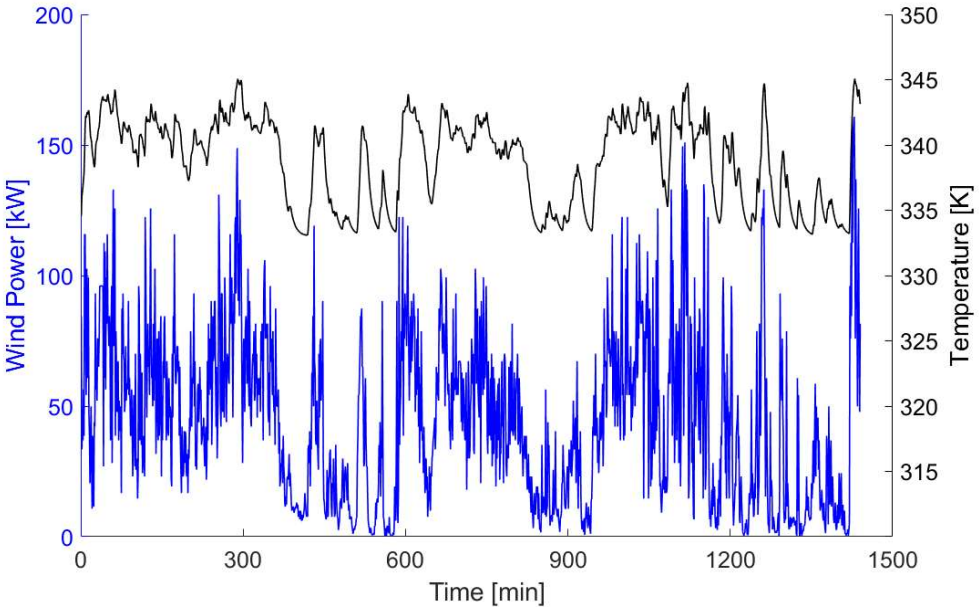

Figure 7. Power from a wind turbine and respective temperature trend during an average day.

Hydrogen production for the two cases of wind power was obtained through the coupled electrochemical-thermal model, as shown in the graphs below.

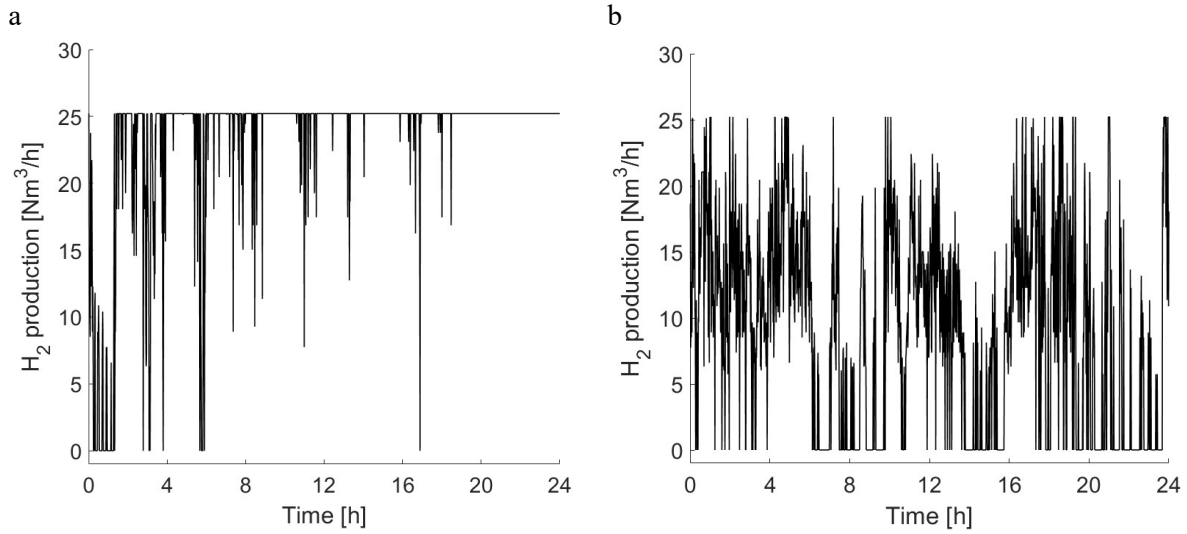

Figure 8. Hydrogen production trend: (a) windy day and (b) average day.

Finally, a comparison between the physics-based model and a simplified model was undertaken. The second one is intended for a user who adopts a simplistic approach without going in detail through the physics of electrolysis, but only using information available from an electrolyzer data sheet.

The simplified model was designed so that it could be taking as input an average production of hydrogen as a result of the power applied. In particular, a producibility of 0.215 Nm³/kWh was applied for the simulation, corresponding to the nominal value from the electrolyzer data sheet. The following graph presents the difference in output, in terms of hydrogen production, between the electrochemical-thermal coupled model and the simplified model.

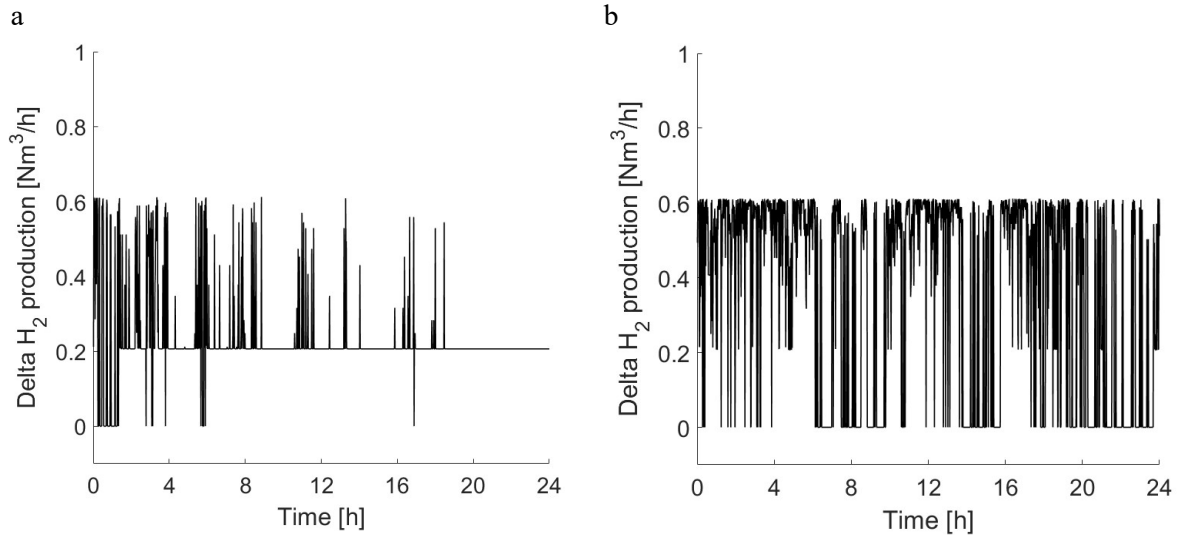

Figure 9. Difference of hydrogen production between coupled and simplified model paired with wind power: (a) windy day and (b) average day.

The difference of hydrogen production between the two models follows the trend of the wind power applied to the stack. Between coupled and simple models the average percentage difference is 1% for the windy day, and 3% for the case of average day. In the second case the electrolyzer works more often in partial conditions and the percentage difference can reach maximum values of 8% for the lowest power inputs.

5. Conclusions

A physics-based model, capable of representing the electrical phenomena involving electrolysis, was developed in Matlab® environment. Thermodynamic and two-phase flow effect were included in the code, following a more comprehensive approach than linear or empirical modeling. Also, a thermal model of the overall system was included and coupled to the electrochemical one, in both steady state and transient cases. Notwithstanding its complexity, the model is relatively lightweight in terms of computational speed, able to account for coupling with renewable energy production systems and the simulation of potential interventions on the device.

The model was applied to a small-size, zero-gap, alkaline electrolyzer and validated through dedicated measurements: good results were obtained concerning the polarization curve (R^2 about 0.9), allowing to identify the membrane as a source of greater overvoltage due to premature deterioration. The hydrogen production calculated and the efficiency obtained, of about 70%, were analogous to the ones expected. The steady-state thermal model of the stack gave good results in terms of electrolyte temperature whereas the transient thermal model including the separators gave a temperature trend consistent with data obtained from tests, with an error of about 0.25%.

Finally, sensitivity analyses were conducted on the models. A change in membrane resistivity was first evaluated, obtaining different polarization curves. The coupled model was applied to a wind turbine power output, to simulate a coupling with the electrolyzer and display the results in terms of electrolyte temperature and hydrogen production. Also, a comparison with a simplified model was performed, showing slight differences, especially at partial loads, i.e. for the lowest values of wind power.

The importance of having a physics-based model is evident. Being independent from a real-case device, differently from empirical modeling, it allows to simulate different systems with changes in material characteristics, geometries and electrical inputs with a more flexible approach.

6. References

[1] International Energy Agency, Global Hydrogen review 2022 https://www.iea.org/reports/global-hydrogen-review-2022
[2] Ritchie H, Roser M, Rosado P, CO_2 and Greenhouse Gas Emissions, 2020, 'https://ourworldindata.org/co2-and-greenhouse-gas-emissions'
[3] Kayfeci M, Keçebaş A, and Bayat M, Solar Hydrogen Production, 2019, Academic Press, Chapter 3, 45-83.
[4] Gutiérrez-Martín F, García-De María J M, Baïri A, Laraqi N, Management strategies for surplus electricity loads using electrolytic hydrogen, 2009, *International Journal of Hydrogen Energy* **34**.
[5] Ursúa A, Sanchis P, Static–dynamic modelling of the electrical behaviour of a commercial advanced alkaline water electrolyser, 2012, *International Journal of Hydrogen Energy* **37**,
[6] Sarrias-Mena R, Fernández-Ramírez L M, García-Vázquez C A, Jurado F, Electrolyzer models for hydrogen production from wind energy systems, 2015, *International Journal of Hydrogen Energy* **40,** 2927-2938.
[7] Tijani A S, Yusup N A B, Abdol Rahim A H, Mathematical modelling and simulation analysis of advanced alkaline electrolyzer system for hydrogen production, 2014, *Procedia Technology* **15**, 798-806.
[8] Vanhanen J P, Lund P D, Computational approaches for improving seasonal storage systems based on hydrogen technologies, 1995, *International Journal of Hydrogen Energy*, **20**, 575-585.
[9] Ulleberg Ø, Modeling of advanced alkaline electrolyzers: a system simulation approach, 2003, *International Journal of Hydrogen Energy* **28**, Issue 1, 21–33.
[10] Zeng K, Zhang D, Recent progress in alkaline water electrolysis for hydrogen production and applications, 2010, *Progress in Energy and Combustion Science*, **36,** 307-326.
[11] Henao C, Agbossou K, Hammoudi M, Dubé Y, Cardenas A, Simulation tool based on a physics model and an electrical analogy for an alkaline electrolyser, 2014, *Journal of Power Sources* **250**, 58-67.
[12] Hammoudi M, Henao C, Agbossou K, Dubé Y, Doumbia M L, New multi-physics approach for modelling and design of alkaline electrolyzers, 2012, *International Journal of Hydrogen Energy* **37**, 13895-13913.
[13] Deshmukh S S, Boehm R F, Review of modeling details related to renewably powered hydrogen systems, 2008, *Renewable and Sustainable Energy Reviews*, **12**, 2301-2330.
[14] Olivier P, Bourasseau C, Bouamama B, Low-temperature electrolysis system modelling: A review, 2017, *Renewable and Sustainable Energy Reviews* **78**, 280-300.
[15] Amores E, Rodrìguez J, Oviedo J, De Lucas Consegruas A, Development of an operation strategy for hydrogen production using solar PV energy based on fluid dynamic aspects, 2017, *Open Engineering* **7**, 141-152.
[16] Prentice G, Encyclopedia of Physical Science and Technology (Third Edition), 2003, 143-159.
[17] LeRoy R L, Bowen C T, and LeRoy D J, The thermodynamics of aqueous water electrolysis, 1980, *Journal of the Electrochemical Society* **127.**
[18] Vogt H, Balzer R J, The bubble coverage of gas-evolving electrodes in stagnant electrolytes, 2005, *Electrochimica acta* **50,** 2073-2079.